JOURNAL OF SOLID STATE CHEMISTRY 51, 53–58 (1984)

Effect of Zirconium Substitution on the Crystallographic and Dielectric Properties of $LiTaO_3$

M. ZRIOUIL AND B. ELOUADI

Applied Solid State Chemistry Laboratory, Department of Chemistry, Faculty of Sciences, Avenue Ibn Batouta, Rabat, Morocco

AND J. RAVEZ AND P. HAGENMULLER

Laboratoire de Chimie du Solide du CNRS, Université de Bordeaux I, 351, cours de la Libération, 33405 Talence Cedex, France

Received July 5, 1983

An investigation of zirconium substitution in the $LiTaO_3$ lattice led to a comprehensive study of several solid solutions in the Li_2O–Ta_2O_5–$(ZrO_2)_2$ phase diagram. Dielectric measurements showed that the nonstoichiometric phases obtained by cation excesses or deficiencies in $LiTaO_3$ were ferroelectric. The Curie temperature decreased when the composition deviated from $LiTaO_3$.

Lithium tantalate is of great interest as a pyroelectric and electrooptical material due to its potential applications: pyroelectric hybrid focal planes, monolitic pyroelectric arrays, commercial saw TV/IF filters, pyroelectric ionization up convectors (*1–6*). The possibility of modulating these properties by cation substitutions has been recently pointed out (*7*). They all lead to a decrease in the Curie temperature of $LiTaO_3$ (t_c = 665°C); for example, 510°C for $Li_{0.873}Ta_{1.025}O_3$ in the Li_2O–Ta_2O_5 system (*8*); 300°C for $Li_{0.80}Ca_{0.20}Ta_{0.80}Zr_{0.20}O_3$ in the $LiTaO_3$–$CaZrO_3$ system (*9*); and 205°C for $Li_{1.14}Ta_{0.86}Ti_{0.14}O_3$ in the Li_2O–Ta_2O_5–$(TiO_2)_2$ ternary diagram (*10*).

Our purpose in this paper was to study the crystallographic and dielectric properties of some nonstoichiometric $LiTaO_3$ derived phases which appear in the Li_2O–Ta_2O_5–$(ZrO_2)_2$ ternary diagram (Fig. 1).

The structure of the ferroelectric room temperature variety of $LiTaO_3$ has been determined by Abrahams *et al.* (*11, 12*). The symmetry is trigonal with space group $R3c$. The cations are localized in two-thirds of the octahedral vacancies of the hexagonal close packed oxygen sublattice.

The Various Theoretical Types of Nonstoichiometry

Figure 1 shows the ternary diagram Li_2O–Ta_2O_5–$(ZrO_2)_2$. The composition lines investigated are drawn on the diagram: lines A ($LiTaO_3$–Li_2O), B ($LiTaO_3$–Li_2ZrO_3), C ($LiTaO_3$–$Li_2Zr_2O_5$), D ($LiTaO_3$–$Li_2Zr_4O_9$), E ($LiTaO_3$–Zr_2O_4), F ($LiTaO_3$–$Ta_2Zr_2O_9$), and G ($LiTaO_3$–Ta_2O_5).

0022-4596/84 $3.00

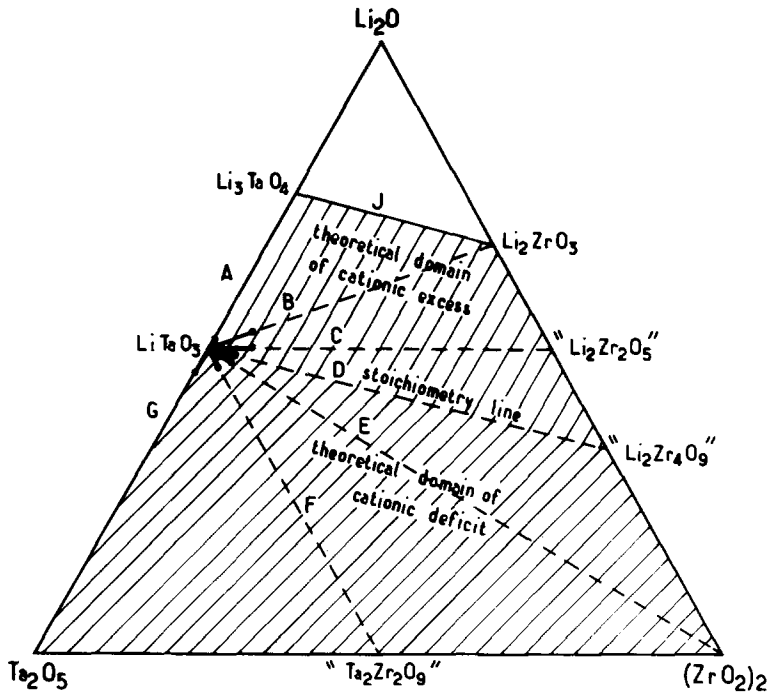

FIG. 1. The various solid solutions studied in the Li_2O–Ta_2O_5–$(ZrO_2)_2$ ternary diagram.

As stoichiometric $LiTaO_3$ contains one cation vacancy for each O_3 set and no anion deficit, four ways can be considered for obtaining nonstoichiometry:

cation excesses from $LiTaO_3$ ($\square_{1-x}M_{2+x}O_3$ ($\square$ = cation vacancies, M = set of atoms in cation sites);

cation deficits ($\square_{1+x}M_{2-x}O_3$;

anion vacancies ($\square M_2O_{3-y}\triangle_y$ ($\triangle$ = anion vacancies);

simultaneous anion vacancies and cation vacancies or cation excesses ($\square_{1\pm x}M_{2\mp x}O_{3-y}\triangle_y$.

Crystal Chemical Study

The materials are prepared from powder mixtures of Li_2CO_3, Ta_2O_5, and ZrO_2 by successive 15-hr heatings at 700 and 1000°C, then 4 hr at 1350°C. The various heat treatments are separated by grinding. Weight measurements before and after each firing allow us to check complete loss of CO_2 and the compositional stability of the sample. The upper limits of each solid solution have been determined by X-ray diffraction (see Fig. 1 and Table I).

To define the type of nonstoichiometry obtained along each line and hence the structural formulation of the various solid solutions, we have investigated the variation of the density vs composition using hydrostatic pressure measurements. They all show that nonstoichiometry appears only either by cation excesses or by cation deficits. Figure 2 gives, for example, the density vs composition variation along line F. From the general theoretical formulation of the line

$$(\square_{1+(n-1)x}Li_{1-x}Ta_{\frac{1+1-n}{2}x}Zr_{\frac{3-n}{2}x}O_{3-3/4(3n-5)x}\triangle_{3/4(3n-5)x},$$

where $\square$ = cation vacancy; $\triangle$ = anionic

TABLE I

EXPERIMENTAL FORMULAS FOR EACH SOLID SOLUTION IN THE TERNARY DIAGRAM, UPPER COMPOSITION LIMITS, AND CURIE TEMPERATURES OF THE BORDER PHASES

Line	Formulas	No. of cations per unit formula	γ = stoichiometry deviation per unit formula[a]	Upper limit of x	Upper limit of γ for x_{max}	t_c per border phase (°C)
A	$Li_{1+x}Ta_{1-x/5}O_3$	$2 + 4/5x$	$+4/5x$	0.07	0.056	640
B	$Li_{1+x}Ta_{1-x}Zr_xO_3$	$2 + x$	$+x$	0.12	0.12	345
C	$Li_{1+x}Ta_{1-5x}Zr_{6x}O_3$	$2 + 2x$	$+2x$	0.02	0.04	375
D	$Li_{1-x}Ta_{1-3x}Zr_{4x}O_3$	2	0	0.02	0	590
E	$Li_{1-x}Ta_{1-x}Zr_{3/2x}O_3$	$2 - x/2$	$-x/2$	−0.06	−0.03	580
F	$Li_{1-x}Ta_{1-x/3}Zr_{2/3x}O_3$	$2 - 2/3x$	$-2/3x$	−0.09	−0.06	545
G	$Li_{1-x}Ta_{1+x/5}O_3$	$2 - 4/5x$	$-4/5x$	−0.12	−0.096	485

[a] $\gamma > 0$ for cation excesses; $\gamma < 0$ for cation deficits.

vacancy; and n = total number of cationic vacancies, it is obvious that the nonstoichiometry is of the cationic deficit type (Fig. 2). As $n = 5/3$ we detect $2x/3$ cationic vacancies per unit formula; there is no anionic deficit.

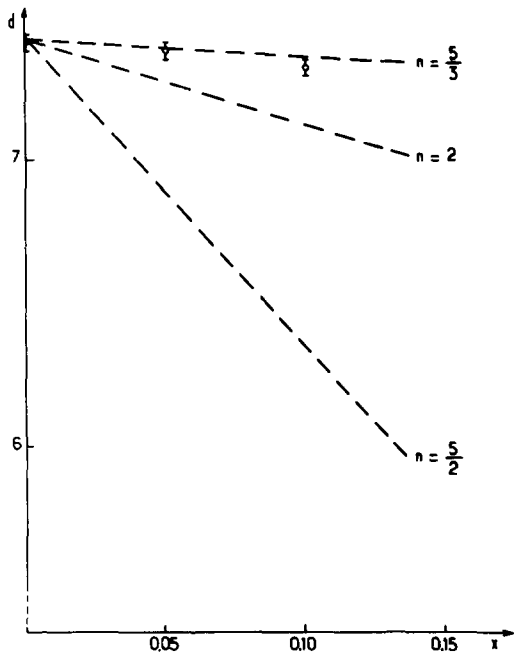

FIG. 2. Variation of the calculated and experimental densities versus composition for line F: $\square_{1+(n-1)x}Li_{1-x}Ta_{2+[(1-n)/2)/2]x}Zr_{[(3-n)/2]x}O_{3-3/4(3n-5)x}\triangle_{3/4(3n-5)x}$ where $\square$ = cationic deficit, A = anionic deficit, and n = number of cationic defects, which may vary from 0 to 3.

The ternary diagram may be thus divided into four domains (Fig. 1):

the triangle Li_2O–Li_3TaO_4–Li_2ZrO_3 (except line J) cannot contain any solid solution since the whole area corresponds to a ratio

$$\alpha = \frac{\text{cation number}}{\text{anion number}} > 1$$

(one has to remember that the highest possible value of α is 1);

the domain including lines A, B, and C correspond to a cation excess from the $LiTaO_3$ composition, but with $\alpha < 1$;

line D which has the same stoichiometry as pure $LiTaO_3$ ($\alpha = \frac{2}{3}$);

the domain including lines E, F, and G which corresponds to cationic deficit from $LiTaO_3$ ($\alpha < \frac{2}{3}$).

The resulting formulas obtained are grouped in Table I. The value of γ can be defined as the difference between the number of cations per unit formula existing in each solid solution and those observed in $LiTaO_3$ for which $\gamma = 0$. As the formulation is $M_{2+\gamma}O_3$, $\alpha = (2 + \gamma)/3$.

All our solid solutions have a trigonal

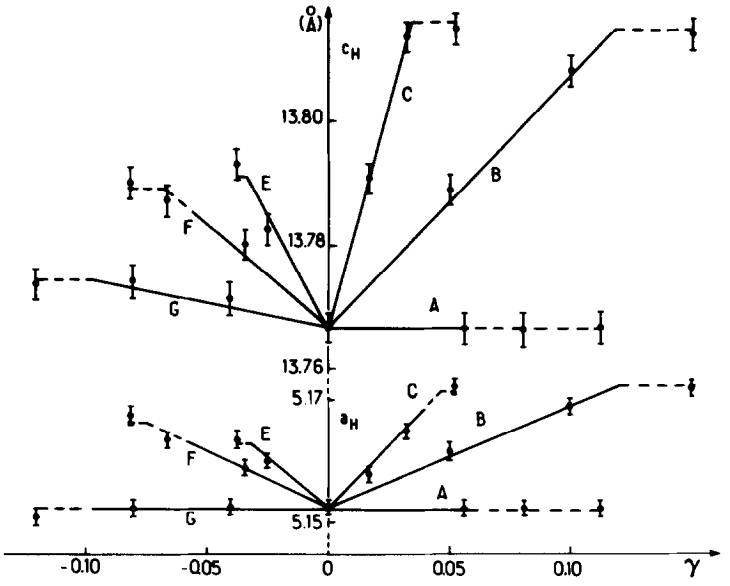

FIG. 3. Variation of the unit cell parameters of the various solid solutions vs γ at 25°C.

symmetry with a $LiTaO_3$-related structure. Figure 3 represents the variation of the hexagonal unit cell parameters vs γ. The a_H and c_H parameters all increase when zirco-

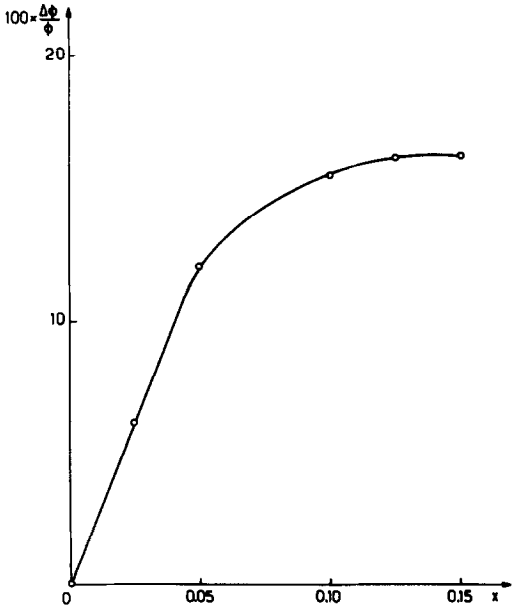

FIG. 4. Diameter shrinkage of sample disk vs composition for compositions along line B.

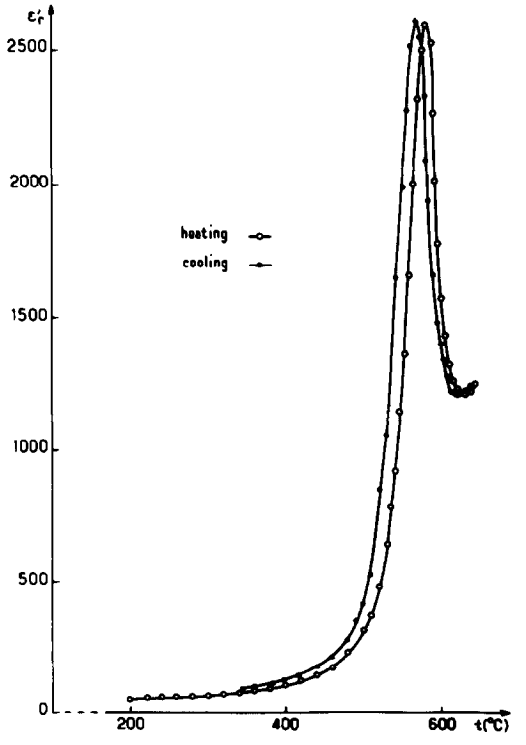

FIG. 5. Thermal variation of ε'_r for a ceramic with $Li_{0.925}Ta_{0.975}Zr_{0.050}O_3$ composition (1 kHz).

nium is introduced in the $LiTaO_3$ lattice. This increase results from the increase of the cation size as Li^+ and Ta^{5+} are substituted by Zr^{4+} ($r_{Li^+} = 0.68$ Å, $r_{Ta^{5+}} = 0.68$ Å, and $r_{Zr^{4+}} = 0.79$ Å with C.N. 6) (*14*).

Dielectric Study

Ceramic samples have been prepared by sintering pressed pellets at 1350°C under an oxygen atmosphere. For many samples the disk diameter after firing decreased as the composition deviated from $LiTaO_3$. Figure 4 illustrates diameter shrinkage vs composition for compositions along line B. This indicates that the sintering temperatures and hence the melting points decrease when the sample deviates from $LiTaO_3$. This property seems very attractive for crystal growth.

Electrodes were deposited on the circular faces using a silver paste. Dielectric measurements were performed at 1 kHz frequency from room temperature to 750°C. For each material the thermal variation of the permittivity ε_r' shows a maximum which can be attributed to the ferroelectric–paraelectric transition. Figure 5 gives the $\varepsilon_r'(t)$ curves obtained by heating and cooling a ceramic corresponding to $x = 0.075$ on line F.

The variation of the ferroelectric Curie temperature t_c vs γ along the considered lines of the diagram is represented in Fig. 6.

Discussion and Conclusion

A crystal chemical study has allowed us to identify some new nonstoichiometric materials with a $LiTaO_3$-related structure. Their compositions are close to that of $LiTaO_3$ in the Li_2O–Ta_2O_5–$(ZrO_2)_2$ diagram. The type of nonstoichiometry (either cationic excess or cationic deficit) has been determined by density measurements.

Each material shows a ferroelectric–paraelectric transition, the Curie temperature t_c decreasing from $LiTaO_3$ for each solid solution considered. This result can be explained by the increasing cation size when replacing Li^+ and Ti^{4+} by Zr^{4+} which causes a smaller cation shift into the octahedral sites comparatively to $LiTaO_3$. The maximum decrease of the Curie temperature is observed when going from 665°C for $LiTaO_3$ to 345°C for $Li_{1.12}Ta_{0.88}Zr_{0.12}O_3$ (line

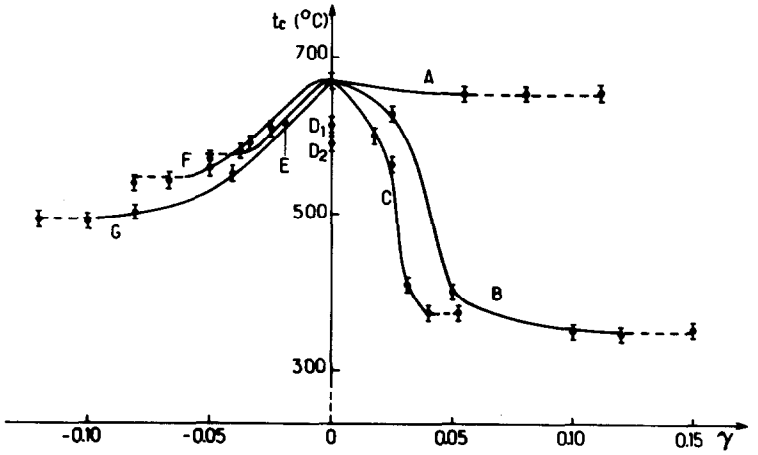

FIG. 6. Variation of the Curie temperature vs γ along the considered lines of the ternary diagram. The values of D_1 and D_2 correspond, respectively, to $x = 0.013$ and $x = 0.020$ for compositions along line D.

B). The diffuse character of the transition, the quality of the ceramics, and the diminution of the melting point make these materials attractive for eventual piezoelectric and pyroelectric applications.

References

1. T. Fukuda, S. Matsumura, H. Hirano, and T. Ito, *J. Cryst. Growth* **46,** 179 (1979).
2. J. Ravez and F. Micheron, *Actual. Chim.* **1,** 9 (1979).
3. S. Iwasa, J. Gelpey, and K. Hartnett, *Ferroelectrics* **27,** 9 (1980).
4. N. E. Byer and A. van der Jagt, *Ferroelectrics* **27,** 11 (1980).
5. H. Hiranoi, *Ferroelectrics* **27,** 151 (1980).
6. N. N. Lebedeva, A. M. Mamedov, A. R. Mardukhaev, and A. Khzenally, *Ferroelectrics* **28,** 363 (1980).
7. R. R. Neurgaonkar, T. C. Lim, E. J. Staples, and L. E. Cross. *Ferroelectrics* **27,** 63 (1980).
8. R. L. Barns and J. R. Carruthers. *J. Appl. Cryst.* **3,** 395 (1970).
9. R. R. Neurgaonkar, T. C. Lim, and E. J. Staples, *Mater. Res. Bull.* **13,** 365 (1978).
10. B. Elouadi, M. Zriouil, J. Ravez, and P. Hagenmuller, *Mater. Res. Bull.* **16,** 1099 (1981).
11. S. C. Abrahams and J. L. Bernstein, *J. Phys. Chem. Solids* **28,** 1685 (1967).
12. S. C. Abrahams, W. C. Hamilton, and A. Sequeira, *J. Phys. Chem. Solids* **28,** 1693 (1967).
13. M. Zriouil, thèse de D.E.S. de 3ème cycle, Rabat, (1981).
14. R. D. Shannon and C. T. Prewitt, *Acta Crystallogr. Sect. B* **25,** 925 (1969).